Proceedings of the
44th IEEE Conference on Decision and Control, and
the European Control Conference 2005
Seville, Spain, December 12-15, 2005

Improved Numerical Integration Method for Power/Power Electronic Systems Based on Three-Point Collocation

A. P. Meliopoulos, *Fellow, IEEE*, George J. Cokkinides, *Senior member, IEEE*, and George K. Stefopoulos, *Student member, IEEE*

Abstract— **This paper presents a new approach for time-domain transient simulation of electric power systems with or without power electronic (switching) subsystems. The new methodology has been named quadratic integration method. The method is based on the following two innovations: (a) the nonlinear system model equations (in general differential-algebraic) are reformulated to a fully equivalent system of quadratic equations, by introducing additional state variables, and (b) the system model equations are integrated assuming that the system states vary quadratically within a time step (quadratic integration).**

The proposed method yields an implicit integration scheme which demonstrates improved convergence characteristics and most importantly improved solution precision. The approach also demonstrates superior behavior compared to traditionally used methods in power system transient analysis (such as the trapezoidal integration rule) in terms of accuracy and numerical stability properties, especially for switching systems. Details about the numerical properties of the method are discussed in the paper.

The proposed methodology and its performance is demonstrated on two test systems including (a) nonlinear R-L electric circuit, and (b) power electronic circuit (switching system). The methodology is very useful for systems with power electronics and nonlinear devices such as saturable transformers/reactors and surge arresters.

I. Introduction

THIS paper presents a new approach for time domain transient simulation of electric power systems with or without power electronic (switching) subsystems. The new methodology has been named quadratic integration method. The method is based on the following two innovations: (a) the nonlinear system-model equations (nonlinear differential or differential-algebraic equations) are reformulated to a fully equivalent system of quadratic equations, by introducing additional state variables and algebraic equations, and (b) the system model equations are integrated using an implicit numerical scheme assuming that the system states vary quadratically within a time step (quadratic integration).

Dynamic simulation is a very important tool in power system transient analysis and therefore a great number of numerical integration methods have been proposed and used for power system time-domain simulation [1-10]. Such methods include backward Euler, Trapezoidal, explicit Runge-Kutta methods, Gear's method, or other linear multistep methods, mainly of the backward differentiation formula (BDF) family. The range of transient phenomena under study in a power systems may vary from fast transients, like lighting stokes, to very slow phenomena like generating unit boiler dynamics. Therefore, the equations describing the operation of a power system are by nature very stiff, i.e. the time constants of the various physical processes vary significantly. In general, very fast transients are studied separately from slow dynamics, nevertheless, in most situations the power system model equations remain stiff and thus implicit integration methods are preferred to explicit, though more expensive in terms of computation time. The simultaneous implicit simulation approach is used in general, in which the algebraic equations are solved along with the discretized differential equations, as a single system, in each time step. Among these methods, the trapezoidal integration is one of the most popular ones in network transient analysis, due to its merits of low distortion and absolute stability (A-stability). For example, the trapezoidal rule is used in EMTP [11-13], Spice [11], and Virtual Test Bed [11].

However, the trapezoidal rule has several drawbacks that limit its applicability and indicate that some improvements in dynamic simulation methods are needed. Two major disadvantages of the trapezoidal integration scheme are its low accuracy compared to other existing methods (trapezoidal rule is order two accurate) and the artificial numerical oscillations that are often encountered, especially in the simulation of power electronic circuits, where switching events, and therefore discontinuities, occur. Specifically, the numerical values of certain variables oscillate around the true values. The magnitude and frequency of such numerical oscillations are directly related to the parameters of the energy storage elements (inductors, capacitors) and the simulation time step. In several cases this problem is so severe that the simulation results are erroneous.

The problem has been extensively studied in the literature

Manuscript received March 7, 2005.

A. P. Meliopoulos is with the School of Electrical and Computer Engineering, Georgia Institute of Technology, Atlanta, GA 30332 USA (phone: 404-894-2926; fax: 404-894-xxxx; e-mail: sakis.meliopoulos@ece.gatech.edu).

G. J. Cokkinides., is with the School of Electrical and Computer Engineering, Georgia Institute of Technology, Atlanta, GA 30332 USA (e-mail: george.cokkinides@ece.gatech.edu).

G. K. Stefopoulos is with the School of Electrical and Computer Engineering, Georgia Institute of Technology, Atlanta, GA 30332 USA (e-mail: gstefop@ece.gatech.edu).

0-7803-9568-9/05/$20.00 ©2005 IEEE

and several solutions have been proposed [11-21] to suppress these numerical oscillations. One popular approach is to use the trapezoidal rule with damping [14]. However, this method introduces artificial elements in the system that may affect the true solution to some extent. Another interesting approach is to apply the critical damping adjustment (CDA) scheme, as proposed in [12] and [13]. This approach suggest to switch from the trapezoidal integration rule to another integration method that does not have an oscillation problem, like backward Euler, for one time step after the discontinuity and then switch back to the trapezoidal rule again and continue the simulation normally. This idea has been extensively studied and several similar approaches of combination of trapezoidal and backward Euler rules have been proposed [15-18]. The Gear's second order method has been proposed as an alternative. The method does eliminate such numerical oscillations; however, it is as accurate as the trapezoidal method, so it does not provide any advantage in terms of accuracy. Furthermore it is not A-stable, which is a desired property. Filter interpolation was used in [20] and a method based on wave digital filters has been also suggested and studied [21].

This paper introduces a new numerical integration method for power system simulation. The method is order four accurate and therefore much more precise compared to all the traditionally used methods in power system applications. Furthermore, the proposed method does not suffer from the numerical oscillation problem, a great advantage as compared to the trapezoidal rule. We refer to this method as quadratic integration method.

II. Description of Quadratic Integration Method

This section presents the key features of the quadratic integration method. The method is based on two innovations: First, the nonlinear system-model equations (nonlinear differential or differential-algebraic equations) are reformulated to a fully equivalent system of quadratic equations, by introducing additional state variables and additional algebraic equations. For implementation purposes the model is transformed to a fully equivalent model of linear differential and quadratic algebraic equations. This step aims in reducing the nonlinearity of the system to at most quadratic in an attempt to improve the efficiency of the solution algorithm. It is independent of the integration method and thus can be applied in combination with any numerical integration rule. Second, the system model equations are integrated using an implicit numerical scheme assuming that the system states vary quadratically within a time step (quadratic integration).

The basic concept of the quadratic integration method is illustrated in Fig. 1. In the trapezoidal rule it is assumed that the system states vary linearly throughout a time step. In this approach it is assumed that they vary quadratically within an integration step. Note that within an integration time step of length h, defined by the interval $[t-h,t]$, the two end points, $x(t-h)$, $x(t)$, and the midpoint x_m $\left(x_m = x(t_m) = x(t-h/2)\right)$ fully define the quadratic function in the interval $[t-h,t]$. Specifically, the quadratic function that passes through the mid and end points is:

$$x(\tau) = a + b\tau + c\tau^2, \qquad 0 \le \tau \le h, \tag{1}$$

where:

$$\begin{aligned} a &= x(t-h), \\ b &= \left(-3x(t-h) + 4x_m - x(t)\right)/h, \\ c &= 2\cdot\left(x(t-h) - 2x_m + x(t)\right)/h^2. \end{aligned} \tag{2}$$

This quadratic function is integrated in the time intervals $[t-h,t_m]$ and $[t-h,t]$ resulting in a set of algebraic equations. For the special case of a linear system

$$\dot{x} = Ax + Bu \tag{3}$$

the algebraic equations at each time step become:

$$\begin{bmatrix} \frac{h}{24}A & I-\frac{h}{3}A \\ I-\frac{h}{6}A & -\frac{2h}{3}A \end{bmatrix}\cdot\begin{bmatrix} x(t) \\ x_m \end{bmatrix} = \begin{bmatrix} \left(I+\frac{5h}{24}A\right) \\ \left(I+\frac{h}{6}A\right) \end{bmatrix}\cdot x(t-h) + \begin{bmatrix} -\frac{h}{24}B & \frac{5h}{24}B & \frac{h}{3}B \\ \frac{h}{6}B & \frac{h}{6}B & \frac{2h}{3}B \end{bmatrix}\cdot\begin{bmatrix} u(t) \\ u(t-h) \\ u_m \end{bmatrix} \tag{4}$$

I is the identity matrix of proper dimension and h the length of the integration time step.

Note that any nonlinear power system or power electronics model can be transformed into a set of linear differential equations and a set of algebraic equations of degree no more than 2 (quadratic) by the introduction of appropriate state variables. Then, the linear differential equations are integrated as discussed above, resulting in an equation similar to (4) above and the quadratic algebraic equations of the system (at times t and t_m) are appended to the set of equations (4). The end result is a model that contains one subset of linear equations and another subset of quadratic equations. This system of equations is solved via Newton's method. The proposed method demonstrates improved convergence characteristics of the iterative solution algorithm.

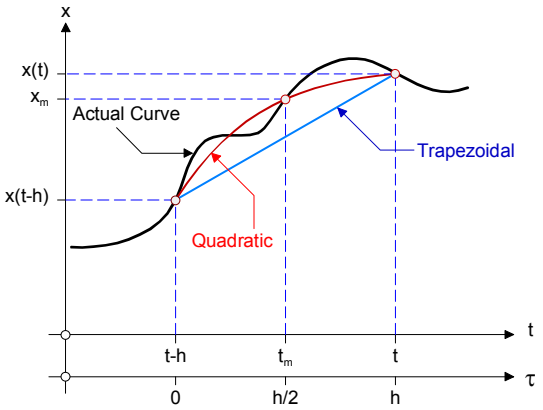

Fig. 1. Illustration of quadratic integration method.

The described quadratic integration method belongs to the category of implicit, Runge-Kutta methods. More specifically it is an implicit Runge-Kutta method based on collocation and it can be derived based on the collocation theory, as described in the Appendix. The basic idea is to

choose a function from a simple space, like the polynomial space, and a set of collocation points, and require that the function satisfy the given problem equations at the collocation points [22-24]. The method has three collocation points, at $x(t-h)$, x_m, and $x(t)$. It uses the Lobatto quadrature rules and is a member of the Lobatto-methods family. Any Lobatto method with s collocation points has an order of accuracy of $2s-2$, and therefore the method is order-four accurate [22-24].

To summarize the method, consider the general nonlinear, non-autonomous dynamical system:

$$\dot{x} = f(t,x), \tag{5a}$$

The system model is quadratized. This is always possible for power system and power electronic systems. Symbolically, the quadratized model is:

$$\dot{x} = h(t,x,y) = A_1 x + A_2 y + Bu(t) \tag{5b}$$
$$0 = g(t,x,y)$$

where $x \in R^n$ is the vector of dynamic states, $y \in R^m$ is a vector of additional state variables, $u \in R^p$ is the input vector, h is a set of linear functions with respect to x and y, and g is a set of quadratic equations. Note the form of the quadratized equations comprises a set of linear differential equations and a set of quadratic algebraic equations. Quadratic integration of the differential equations and appending the algebraic equations yields:

$$\begin{bmatrix} \frac{h}{24}A_1 & \frac{h}{24}A_2 & I_n - \frac{h}{3}A_1 & -\frac{h}{3}A_2 \\ I_n - \frac{h}{6}A_1 & -\frac{h}{6}A_2 & -\frac{2h}{3}A_1 & -\frac{2h}{3}A_2 \end{bmatrix} \cdot \begin{bmatrix} x(t) \\ y(t) \\ x_m \\ y_m \end{bmatrix} = \tag{6}$$
$$\begin{bmatrix} I_n + \frac{5h}{24}A_1 & \frac{5h}{24}A_2 \\ I_n + \frac{h}{6}A_1 & \frac{h}{6}A_2 \end{bmatrix} \cdot \begin{bmatrix} x(t-h) \\ y(t-h) \end{bmatrix} + \begin{bmatrix} -\frac{h}{24}B & \frac{5h}{24}B & \frac{h}{3}B \\ \frac{h}{6}B & \frac{h}{6}B & \frac{2h}{3}B \end{bmatrix} \cdot \begin{bmatrix} u(t) \\ u(t-h) \\ u_m \end{bmatrix}$$
$$0 = g(t, x(t), y(t))$$
$$0 = g(t_m, x_m, y_m)$$

Solution of the above system (2(m+n) equations in 2(m+n) unknowns) via Newton's method yields the value of the state vector $x(t)$. Note that the value at the midpoint, x_m, is simply an intermediate result and it is discarded at the end of the calculations at each step.

The proposed integration approach has the following advantages: (a) improved accuracy and numerical stability, and (b) free of fictitious numerical oscillations. Details about the numerical properties of the method are discussed next

III. Numerical Properties

As already stated, the order of quadratic integration method is $p = 4$. This means that the error at each time step is $O(h^5)$. As an implicit Runge-Kutta scheme, the method is zero-stable [24]. In Butcher array notation the method is compactly expressed as (see Appendix):

0	0	0	0
1/2	5/24	1/3	-1/24
1	1/6	2/3	1/6
	1/6	2/3	1/6

The numerical stability properties are studied using the first order test equation:

$$\dot{x} = ax. \tag{7}$$

Applying the quadratic integration method yields at each time step:

$$\begin{bmatrix} x(t) \\ x_m \end{bmatrix} = \begin{bmatrix} \left(\frac{12+6ah+a^2h^2}{12-6ah+a^2h^2}\right) \\ \left(\frac{12-0.5a^2h^2}{12-6ah+a^2h^2}\right) \end{bmatrix} x(t-h) \tag{8}$$

and therefore:

$$x(t) = \frac{12+6ah+a^2h^2}{12-6ah+a^2h^2} \cdot x(t-h), \tag{9}$$

where h is the integration step. Setting $z = ah$ yields the characteristic polynomial for the method:

$$R(z) = \frac{z^2+6z+12}{z^2-6z+12} \tag{10}$$

In general $R(z) = 1 + zb^T(I - zA)^{-1}I1$ where the values for A and b can be easily obtained from the Butcher array: $A = \begin{bmatrix} 0 & 0 & 0 \\ 5/24 & 1/3 & -1/24 \\ 1/6 & 2/3 & 1/6 \end{bmatrix}$ is the coefficient matrix of the Runge-Kutta method, and $b = [1/6 \quad 2/3 \quad 1/6]^T$ is the coefficient vector of the method. $I1$ is defined as $I1 = [1,1,...,1]^T$.

The region of absolute stability is given by the set of values z such that $|R(z)| \le 1$. A method is called A-stable if the region of absolute stability in the complex z-plane contains the entire left half plane. This means that independently of the step size $h > 0$, a stable eigenvalue a of the original continuous time system, with $\mathrm{Re}(a) < 0$, will be still represented as a stable mode in the discrete time system, and thus the discrete system mimics accurately the behavior of the original system, in terms of stability. Note that, for the proposed method, if $\mathrm{Re}(z) < 0$ it follows from (10) that $|R(z)| \le 1$. Therefore, the method is A-stable. A contour plot of $|R(z)|$ in the complex z-plane is shown in Fig. 2. The absolute stability region of the method is depicted in Fig. 3.

Note that the absolute stability region is exactly the left-hand half complex plane. This property is called strict (or sometimes symmetrical) A-stability. If the dynamical system under study includes an unstable mode, then, irrespectively of the integration step-size, this mode will remain unstable in the descretized system and the unstable nature of the real

system will be accurately demonstrated [7]. This is not the case for other methods, for example, the backward Euler, or the BDF linear, multi-step methods, where the numerical stability domain extends in the right-hand plane, where $\mathrm{Re}(z) > 0$. In this case, if the real dynamical system includes an unstable mode, this mode could appear as stable for some step size, in the discrete system. This implies that the real unstable phenomenon would be simulated as a stable one. This spurious damping is referred to as hyper stability [7].

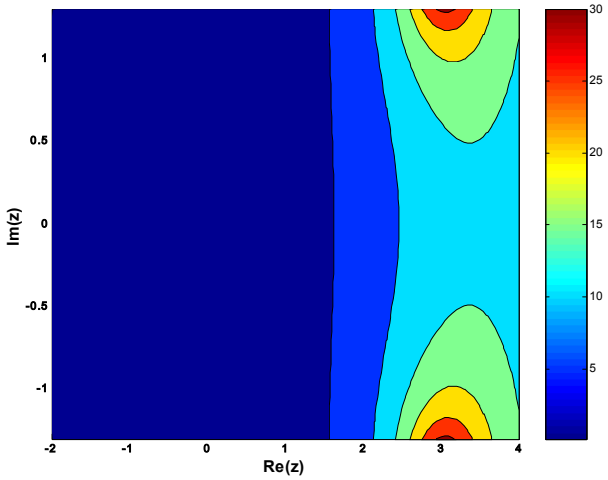

Fig. 2. Contour plot of $|R(z)|$.

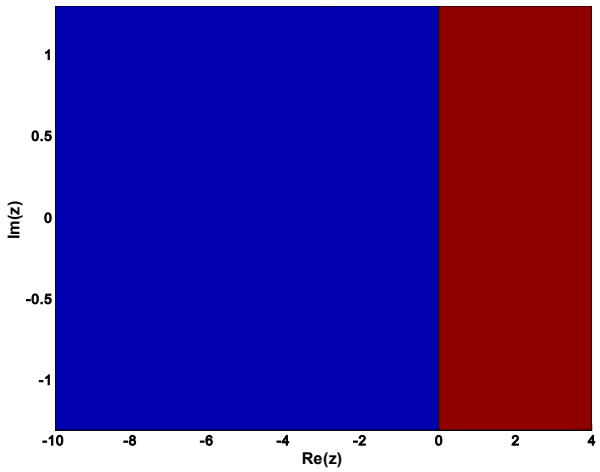

Fig. 3. Absolute stability region of quadratic integration method (left side).

Comparing the quadratic and the trapezoidal integration methods the following hold:

1. Both the trapezoidal method and the quadratic integration method are symmetrical A-stable.
2. The trapezoidal method is order two accurate. The quadratic integration is order four. Therefore, in terms of accuracy, quadratic integration is much preferable.
3. It has been observed in applications that the trapezoidal method can provide an oscillatory solution even for systems that have exponential solutions as the simple test equation above. This is apparent if one considers the characteristic polynomial of the trapezoidal rule $R(z) = \frac{2+z}{2-z}$ for a physically stable system. Note that it is possible to select the integration time step ($z = ah$), so that this term is negative (for example any real value of z, with $z < -2$). This can occur when larger integration steps are selected. In this case the solution will be oscillatory, oscillating around the true solution of the problem. In the case of the quadratic integration, the corresponding term $R(z) = \frac{z^2 + 6z + 12}{z^2 - 6z + 12}$ can never be negative as long as $\mathrm{Re}(z) < 0$, i.e. as long as the physical system is stable. This, indeed, is a very nice characteristic in many applications.

IV. Preliminary Results

This section discusses the application of the method to some preliminary test cases. The examples are purposely simple since the goal is to demonstrate clearly the application and the advantages of the methodology.

A. Nonlinear inductor

The first test-case is an RL circuit with a nonlinear inductor. Two cases of nonlinear inductor are studied: (a) an inductor with a high order nonlinear flux-current characteristic, and (b) a piecewise linear inductor with two linear segments. The circuit in both cases is as in Figure 4. The voltage source is a sinusoidal AC source of 60 Hz and of 10 V rms.

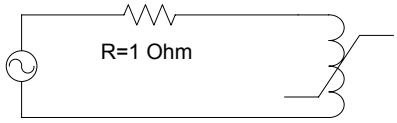

Fig. 4. RL circuit with nonlinear inductor

1) High-order nonlinear inductor

The circuit equations are:

$$\frac{d\lambda}{dt} = -R \cdot i + V_{AC}, \tag{11}$$

where λ is the inductor flux and i the inductor current. The nonlinear characteristic of the inductor is

$$i = i_0 \cdot \left(\frac{\lambda}{\lambda_0}\right)^8 \cdot \mathrm{sgn}(\lambda) \cdot \tag{12}$$

The proposed method consists of quadratization of the equations first and then application of the quadratic integration. The equivalent quadratic system with linear differential and quadratic algebraic equations is (note the introduction of two additional variables, z_1 and z_2 and two additional equations):

$$\begin{aligned} \frac{d\lambda}{dt} &= -R \cdot i + V_{AC} \\ 0 &= i - i_0 \cdot z_2^2 \cdot \mathrm{sgn}(\lambda) \cdot \\ 0 &= \lambda_0^2 \cdot z_1 - \lambda^2 \\ 0 &= z_2 - z_1^2 \end{aligned} \tag{13}$$

Fig. 5 illustrates the computed inductor voltage and current waveforms using the quadratic integration, with a time step of 10 μs. The system parameters are $i_0 = 10\,A$ and $\lambda_0 = 0.03\,Wb$.

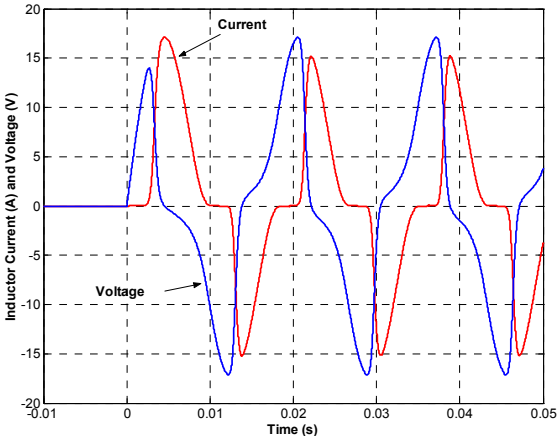

Fig. 5. Inductor voltage and current waveforms of a nonlinear inductor using quadratic integration.

2) Piecewise linear inductor

In this case the circuit equations are:

$$\frac{di}{dt} = \begin{cases} -\frac{R}{L_1}\cdot i + \frac{1}{L_1}\cdot V_{AC}, |i| \le i_0 \\ -\frac{R}{L_2}\cdot i + \frac{1}{L_2}\cdot V_{AC}, |i| \ge i_0 \end{cases} \quad (14)$$

The inductance values are $L_1 = 1\,mH$ and $L_2 = 0.1\,\mu H$. The switching occurs at $i_0 = 12\,A$. Figures 6 and 7 show the waveforms of the inductor voltage and current when computed using the trapezoidal rule with a time step of 10 μs. Note that the results contain numerical oscillations when switching from the first to the second model. Figures 8 and 9 show the same voltage and current waveforms when the system is simulated using quadratic integration with the same time step. Note that the oscillations are eliminated, when this method is used.

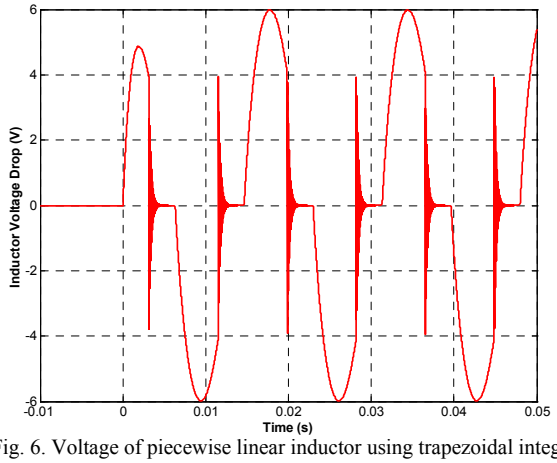

Fig. 6. Voltage of piecewise linear inductor using trapezoidal integration.

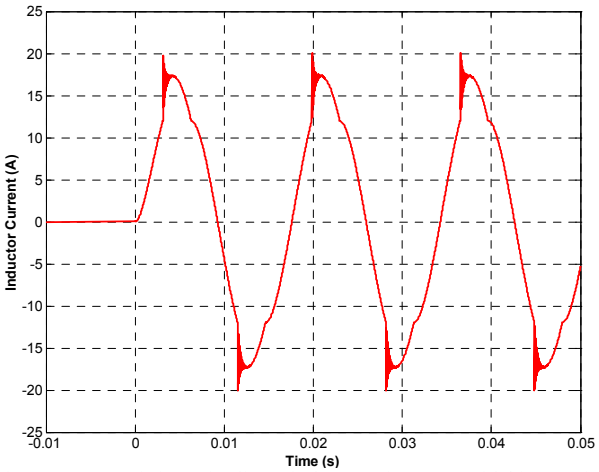

Fig. 7. Current of piecewise linear inductor using trapezoidal integration.

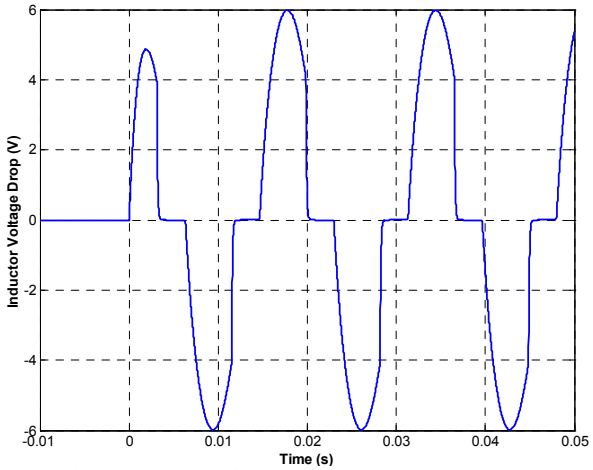

Fig. 8. Voltage of piecewise linear inductor using quadratic integration.

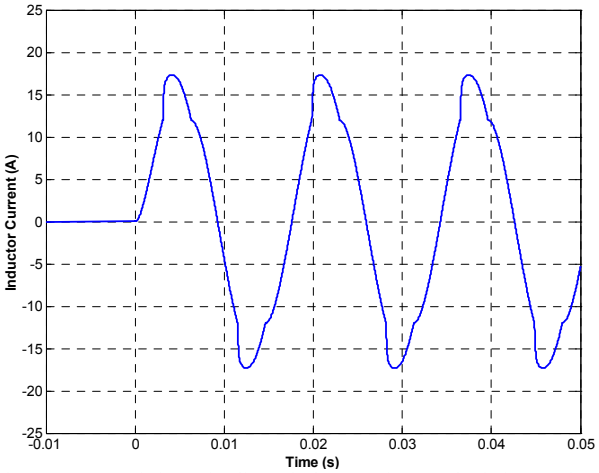

Fig. 9. Current of piecewise linear inductor using quadratic integration.

B. R-L circuit with diode

The second test case is a simple switching system, as illustrated in Figure 10. A sinusoidal voltage source of 10 V rms and 60 Hz frequency drives an inductive load through a diode. This scenario is often encountered in the simulation of power electronic systems. The diode is modeled using a piecewise linear model, as described by (15).

$$i_D = \begin{cases} \dfrac{1}{R_D} \cdot v_D, & v_D \le V_{D0} \\ \dfrac{1}{r_D} \cdot v_D + V_{D0} \cdot \left(\dfrac{1}{R_D} - \dfrac{1}{r_D} \right), & v_D \ge V_{D0} \end{cases} \quad (15)$$

where i_D and v_D are the diode current and voltage respectively. V_{D0} is the diode voltage at which the diode starts conducting and R_D and r_D are the diode resistances. The numerical values of the above constant are:

$R_D = 10^6\ Ohm$, $r_D = 10^{-1}\ Ohm$, $V_{D0} = 0.7\,V$

The inductance value is $L = 1\,mH$. Using the diode voltage as state variable the system equations are:

$$\frac{dv_D}{dt} = \begin{cases} -\dfrac{R + R_D}{L} \cdot v_D + \dfrac{R_D}{L} \cdot V_{AC} & , v_D \le V_{D0} \\ -\dfrac{R + r_d}{L} v_D + \dfrac{r_D}{L} \cdot V_{AC} + \dfrac{V_{D0}}{L} \left((R + r_d)\left(1 - \dfrac{r_D}{R_D}\right) + r_D \left(1 + \dfrac{r_D}{R_D}\right) \right) & , v_D > V_{D0} \end{cases} \quad (16)$$

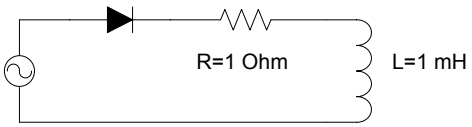

Fig. 10. RL circuit with diode.

Figures 11 and 12 show the diode voltage and current as computed with the trapezoidal integration method with a time step of 2 μs. Figures 13 and 14 show the diode voltage and current as computed with the proposed integration method with a time step of 2 μs (same as in the case of trapezoidal nitration). Note that when the trapezoidal integration is used severe numerical oscillations appear each time the diode is turned off. The quadratic integration successfully eliminates these oscillations.

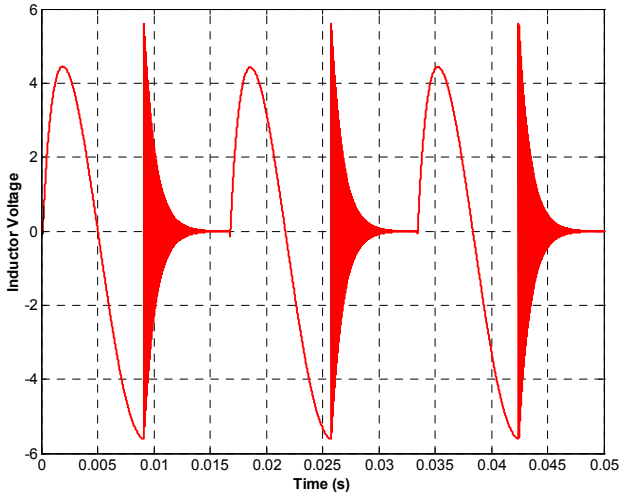

Fig. 11. Inductor voltage using trapezoidal integration.

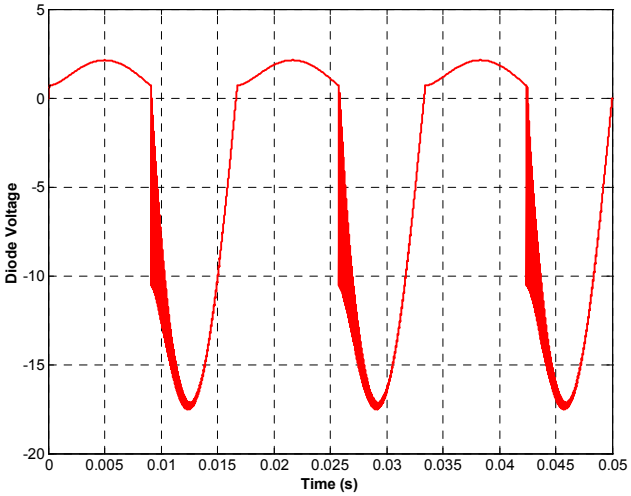

Fig. 12. Diode voltage using trapezoidal integration.

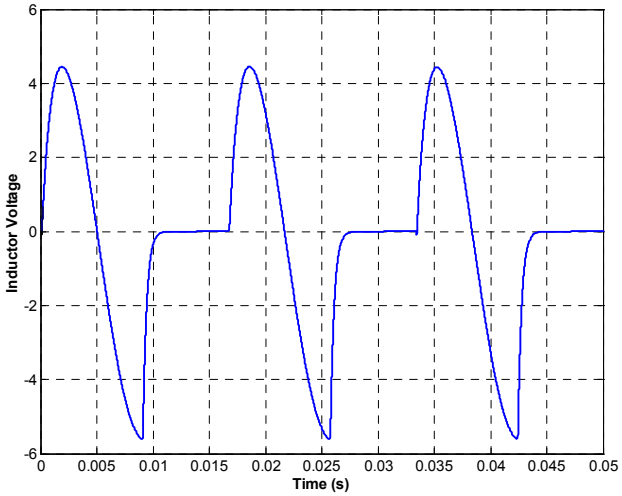

Fig 13. Inductor voltage using quadratic integration.

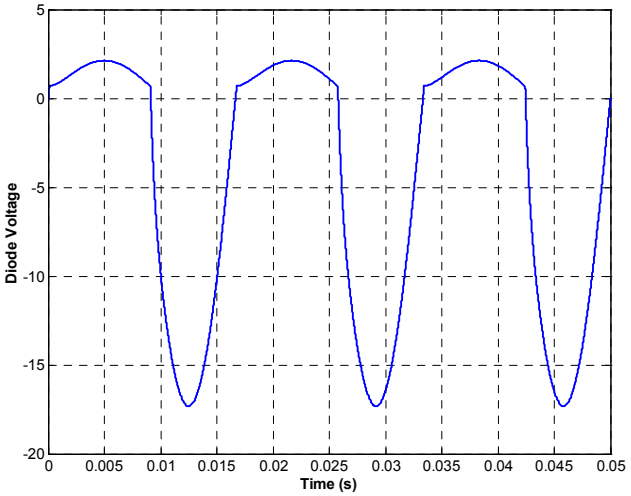

Fig. 14. Diode voltage using quadratic integration.

V. Conclusions And Further Work

This paper introduced some preliminary concepts on a new numerical integration method for power system and power electronic time-domain simulation. The method is

order four accurate and, therefore, much more precise compared to other traditionally used method in this area. Furthermore, the method does not suffer from sustained numerical oscillations after discontinuities (switching events) as the popular trapezoidal integration method. Several simple test cases show that the methodology appears to be a superior and attractive alternative for simulation of power system transients.

The paper focuses on basic concepts and some introductory work on the issue. The numerical properties of the method are presently under study with more thorough evaluation on a number of problems arising in power systems and power electronics. Furthermore, the method is suitable for implementation with variable time step and error estimation and control algorithms. The proposed methodology can be also augmented with singularity detecting algorithms to allow tracking of switching events. Finally we are developing test cases of complex and large scale systems. These test cases will be utilized to study the performance of the methodology in large complex systems. It is expected to report on this work in a future paper.

VI. Appendix

Derivation of quadratic integration method based on collocation rules[24].

Assume the general nonlinear, non-autonomous ordinary differential equation (ODE) $\dot{x} = f(t,x)$, where x is the state vector. Assume three collocation points ($s=3$) defined as $c_1 = 0$, $c_2 = 1/2$, $c_3 = 1$. We seek a polynomial (vector) $\phi(\tau)$ of degree at most $s=3$ which collocates the ODE in [t-h,t] as follows:

$$\begin{aligned}
&\phi(t-h) = x(t-h),\\
&\dot{\phi}(t_1) = \dot{\phi}(t-h) = f\left(t-h,\phi(t-h)\right),\\
&\dot{\phi}(t_2) = \dot{\phi}(t-h/2) = \dot{\phi}(t_m) = f\left(t_m,\phi(t_m)\right),\\
&\dot{\phi}(t_3) = \dot{\phi}(t) = f\left(t,\phi(t)\right),
\end{aligned} \tag{A.1}$$

where t_m=t-h/2 is the midpoint of the integration interval [t-h,t]. Note that these four equations fully define the polynomial vector ϕ.

Define:

$$\begin{aligned}
&K_1 = \dot{\phi}(t_1) = \dot{\phi}(t-h),\\
&K_2 = \dot{\phi}(t_2) = \dot{\phi}(t_m),\\
&K_3 = \dot{\phi}(t_3) = \dot{\phi}(t).
\end{aligned} \tag{A.2}$$

Now we can write $\dot{\phi}$ as a Lagrange interpolation formula

$$\begin{aligned}
\dot{\phi}(t-h+\tau h) &= \sum_{j=1}^{3} L_j(t-h+\tau h)K_j \\
&= L_1(t-h+\tau h)K_1 + L_2(t-h+\tau h)K_2 + L_3(t-h+\tau h)K_3,
\end{aligned} \tag{A.3}$$

where $L_j(t-h+\tau h) = \prod_{i=1,i\neq j}^{s} \frac{(\tau - c_i)}{(c_j - c_i)}$, i.e.:

$$L_1(t-h+\tau h) = \frac{(\tau-c_2)}{(c_1-c_2)}\cdot\frac{(\tau-c_3)}{(c_1-c_3)} = 2\tau^2 - 3\tau + 1,$$

$$L_2(t-h+\tau h) = \frac{(\tau-c_1)}{(c_2-c_1)}\cdot\frac{(\tau-c_3)}{(c_2-c_3)} = -4\left(\tau^2-\tau\right), \tag{A.4}$$

$$L_3(t-h+\tau h) = \frac{(\tau-c_1)}{(c_3-c_1)}\cdot\frac{(\tau-c_2)}{(c_3-c_2)} = 2\tau^2 - \tau\cdot$$

Integrating $\dot{\phi}$ with respect to t from $t-h$ to t_i, $i=1,2,3$, and from $t-h$ to t, we get

$$\begin{aligned}
\phi(t_1) - \phi(t-h) &= h\sum_{j=1}^{3}\left(\int_0^0 L_j(r)dr\right)K_j,\\
\phi(t_2) - \phi(t-h) &= h\sum_{j=1}^{3}\left(\int_0^{1/2} L_j(r)dr\right)K_j,\\
\phi(t_3) - \phi(t-h) &= h\sum_{j=1}^{3}\left(\int_0^1 L_j(r)dr\right)K_j,\\
\phi(t) - \phi(t-h) &= h\sum_{j=1}^{3}\left(\int_0^1 L_j(r)dr\right)K_j.
\end{aligned} \tag{A.5}$$

Note that the first equation vanishes since it is just an identity and the last two coincide. Therefore, the second and third equations are left, which can be written as:

$$\begin{aligned}
\phi(t_m) - \phi(t-h) &= h\sum_{j=1}^{3}\left(\int_0^{1/2} L_j(r)dr\right)K_j,\\
\phi(t) - \phi(t-h) &= h\sum_{j=1}^{3}\left(\int_0^1 L_j(r)dr\right)K_j.
\end{aligned} \tag{A.6}$$

Now define

$$a_{11} = \int_0^{c_1} L_1(r)dr = \int_0^0 L_1(r)dr = 0, \tag{A.7}$$

$$a_{12} = \int_0^{c_1} L_2(r)dr = \int_0^0 L_2(r)dr = 0, \tag{A.8}$$

$$a_{13} = \int_0^{c_1} L_3(r)dr = \int_0^0 L_3(r)dr = 0, \tag{A.9}$$

$$a_{21} = \int_0^{c_2} L_1(r)dr = \int_0^{1/2}\left(2r^2-3r+1\right)dr = \frac{5}{24}, \tag{A.10}$$

$$a_{22} = \int_0^{c_2} L_2(r)dr = -4\int_0^{1/2}\left(r^2-r\right)dr = \frac{1}{3}, \tag{A.11}$$

$$a_{23} = \int_0^{c_2} L_3(r)dr = \int_0^{1/2}\left(2r^2-r\right)dr = -\frac{1}{24}, \tag{A.12}$$

$$a_{31} = \int_0^{c_3} L_1(r)dr = \int_0^{1}\left(2r^2-3r+1\right)dr = \frac{1}{6}, \tag{A.13}$$

$$a_{32} = \int_0^{c_3} L_2(r)dr = -4\int_0^{1}\left(r^2-r\right)dr = \frac{2}{3}, \tag{A.14}$$

$$a_{33} = \int_0^{c_3} L_3(r)dr = \int_0^{1}\left(2r^2-r\right)dr = \frac{1}{6}, \tag{A.15}$$

$$b_1 = \int_0^{1}\left(2r^2-3r+1\right)dr = \frac{1}{6}, \tag{A.16}$$

$$b_2 = -4\int_0^1 \left(r^2 - r\right)dr = \frac{2}{3}, \tag{A.17}$$

$$b_3 = \int_0^1 \left(2r^2 - r\right)dr = \frac{1}{6}. \tag{A.19}$$

Therefore, the Butcher array notation of the method is:

0	0	0	0
1/2	5/24	1/3	-1/24
1	1/6	2/3	1/6
	1/6	2/3	1/6

Using these definitions we have:

$$\begin{aligned} \phi(t_m) - \phi(t-h) &= h\sum_{j=1}^{3} a_{2j}K_j \\ \phi(t) - \phi(t-h) &= h\sum_{j=1}^{3} a_{3j}K_j = h\sum_{j=1}^{3} b_j K_j \end{aligned} \tag{A.20}$$

where

$$\begin{aligned} K_1 &= \dot{\phi}(t-h) = f\left(t-h, \phi(t-h)\right), \\ K_2 &= \dot{\phi}(t_m) = f\left(t_m, \phi(t_m)\right), \\ K_3 &= \dot{\phi}(t) = f\left(t, \phi(t)\right). \end{aligned} \tag{A.21}$$

Therefore the quadratic integration is defined by the following system of equations:

$$\begin{aligned} \phi(t_m) - \phi(t-h) &= \frac{5h}{24} f\left(t-h, \phi(t-h)\right) + \frac{h}{3} f\left(t_m, \phi(t_m)\right) - \frac{h}{24} f\left(t, \phi(t)\right) \\ \phi(t) - \phi(t-h) &= \frac{h}{6} f\left(t-h, \phi(t-h)\right) + \frac{2h}{3} f\left(t_m, \phi(t_m)\right) + \frac{h}{6} f\left(t, \phi(t)\right) \end{aligned} \tag{A.22}$$

The values of ϕ at the various stages represent the estimated values of the unknown state x and based on the collocation is also holds that $\phi(t-h) = x(t-h)$. Thus we can change our notation from ϕ to x and the method becomes:

$$\begin{aligned} x_m - \frac{h}{3} f(t_m, x_m) + \frac{h}{24} f(t, x(t)) &= x(t-h) + \frac{5h}{24} f(t-h, x(t-h)) \\ x(t) - \frac{2h}{3} f(t_m, x_m) - \frac{h}{6} f(t, x(t)) &= x(t-h) + \frac{h}{6} f(t-h, x(t-h)) \end{aligned} \tag{A.23}$$

REFERENCES

[1] H. W. Dommel, "Digital computer simulation of electromagnetic transients in single- and multiphase networks," *IEEE Trans. on Power Apparatus and Systems*, vol. PAS-88, no. 4, pp. 388-399, Apr. 1969.

[2] R. B. I. Johnson, B. J. Cory and M. J. Short, "A tunable integration method for the simulation of power system dynamics," *IEEE Trans. on Power Systems*, vol. 3, no. 4, pp. 1530-1537, Nov. 1988.

[3] K. K. Yen, Z. Hu and J. Andrian, "Stability study of parallel predictor-corrector numerical integration algorithm and redesign," *in.1989 IEEE Energy and Information Technologies in the Southeast Conf.*, vol. 2, pp. 417-420, 9-12 April 1989.

[4] P. P. J. van den Bosch and H. R. Visser, "Simulation of state-events in power electronic devices," *in Proc. of the 4th Int. Conf. on Power Electronics and Variable-Speed Drives*, pp. 184-189, 17-19 July 1990.

[5] T. Kato and K. Ikeuchi, "Variable order and variable step-size integration method for transient analysis programs," *IEEE Trans. on Power Systems*, vol. 6, no. 1, pp. 206-213, Feb. 1991.

[6] T. Kato and T. Kataoka, "Computer-aided analysis of a power electronic circuit by a new multirate method," in *Proc. of the 29th Annual IEEE Power Electronics Specialists Conference(PESC 98)*, vol. 2 pp. 1076-1083, May 1998.

[7] J. Y. Astic, A. Bihain, and M. Jerosolimskii, "The mixed Adams-BDF variable step size algorithm to simulate transient and long term phenomena in power systems," *IEEE Trans. on Power Systems*, vol. 9, no. 2, pp. 929-935, May 1994.

[8] H. Takano, S. M. Ulhaq and M. Nakaoka, "Computer-aided simulation technique of digitally controlled switched-mode power conversion circuits and systems using state variable matrices," *in Proc. of the 1997 Power Conversion Conference*, vol. 1, pp. 411-418, 3-6 Aug. 1997.

[9] P. Pejovic, D. Maksimovic, "PETS-A simulation tool for power electronics," *1996 IEEE Workshop on Computers in Power Electronics*, 11-14 Aug. 1996, pp. 1-8.

[10] V. R. Dinavahi, M. R. Iravani and R. Bonert, "Real-time digital simulation of power electronic apparatus interfaces with digital controllers," *IEEE Trans. on Power Delivery*, vol. 16, no. 4, pp. 775-781, Oct. 2001.

[11] W. Gao, E. Solodovnik, R. Dougal, G. Cokkinides, and A. P. Meliopoulos, "Elimination of numerical oscillations in power system dynamic simulation," in *Proc. of the 18th Annual IEEE Applied Power Electronics Conf. and Exposition (APEC '03)*, vol. 2, pp. 790-794, 9-13 Feb. 2003.

[12] J. R. Marti and J. Lin, "Suppression of numerical oscillations in the EMTP," *IEEE Trans. on Power Systems*, vol. 4, no. 2, pp. 739-747, May 1989.

[13] J. Lin and J. R. Marti, "Implementation of the CDA procedure in the EMTP," *IEEE Trans. on Power Systems*, vol. 5, no. 2, pp. 394-402, May 1990.

[14] F. L. Alvarado, R. H. Lasseter, and J. J. Sanchez, "Testing of trapezoidal integration with damping for the solution of power transient problems," *IEEE Trans. on Power Apparatus and Systems*, vol. PAS-102, no. 12, pp. 3783-3790, Dec. 1983.

[15] K. Strunz, "Position variant integration in digital real time simulators for electromagnetic transients," *in Proc. of the 2002 Int. Conf. on Power System Technology (PowerCon 2002)*, vol. 4, pp. 2019-2025, 13-17 Oct. 2002.

[16] K. Strunz, "Flexible numerical integration for efficient representation of switching in real time electromagnetic transients simulation," *IEEE Trans. on Power Delivery*, vol. 19, no. 3, pp. 1276-1283, July 2004.

[17] K. Strunz, "Position-dependent control of numerical integration in circuit simulation," *IEEE Trans. on Circuits and Systems II: Express Briefs [see also Circuits and Systems II: Analog and Digital Signal Processing]*, vol. 51, issue 10, pp. 561-565, Oct. 2004.

[18] K. Strunz, *Numerical methods for real time simulation of electromagnetics in AC/DC network systems.* Dusseldorf, Germany: VDI Verlag, 2002.

[19] C.-T. Liu and W.-L. Chang, "Synchronized solution of power electronics system equations using flexible MODELS component connected to the EMTP," *IEEE Trans. on Power Delivery*, vol. 11, no. 4, pp. 1868-1873, Oct. 1996.

[20] X. Cao, A. Kurita, T. Yamanaka, Y. Tada and H. Mitsuma, "Suppression of numerical oscillation caused by the EMTP-TACS interface using filter interpolation," *IEEE Trans. on Power Delivery*, vol. 11, no. 4, pp. 2049-2055, Oct. 1996.

[21] M. Roitman and P. S. R. Diniz, "Simulation of non-linear and switching elements for transient analysis based on wave digital filters," *IEEE Trans. on Power Delivery*, vol. 11, no. 4, pp. 2042-2048, Oct. 1996.

[22] E. Hairer, S. P. Norsett and G. Wanner, *Solving ordinary differential equations I: Nonstiff problems*. 2nd ed., New York: Springer-Verlag, 1993.

[23] E. Hairer and G. Wanner, *Solving ordinary differential equations II: Stiff and differential-algebraic problems*. 2nd ed., New York: Springer-Verlag, 1996.

[24] U. M. Ascher and L. R. Petzold, *Computer methods for ordinary differential and differential-algebraic equations*. Society for Industrial and Applied Mathematics (SIAM), 1998.